

Excitation and decay of analogs of excited states of $^{119}\text{Sn}^\dagger$

D. H. Fitzgerald,* J. S. Lilley,[†] and C. H. Poppe[§]

Department of Physics, University of Minnesota, Minneapolis, Minnesota 55455

S. M. Grimes

Lawrence Livermore Laboratory, Livermore, California 94550

(Received 21 March 1978)

The (p, n') reaction to excited isobaric analog states of ^{119}Sn has been observed using a neutron-proton $(n-p)$ coincidence technique. The $n-p$ coincidence was essential to reduce the neutron background due to population of the $T_<$ states. The states preferentially excited are analogs of the 0.920, 0.921, 1.090, and 1.354 MeV states of ^{119}Sn which contain the strength of the 2^+ core excitation. These states are observed to decay overwhelmingly to the first-excited (2^+) state of ^{118}Sn . A value for the overall relative proton decay probability was calculated in order to compare the data with predictions of a two-step model of the (p, n') reaction. Good agreement with the data was obtained, provided that the imaginary part of the neutron optical potential was reduced by the same factor which previously was found necessary to fit quasi-elastic scattering data.

NUCLEAR REACTIONS $^{119}\text{Sn}(p, n')^{119}\text{Sb}(\text{IAS})$, $E_p = 17, 19$ MeV; measured $\sigma(E_p, \theta)$; observed proton decays, obtained two-step DWBA and coupled-channels predictions.

I. INTRODUCTION

During the past 15 years, the (p, n) reaction to analogs of the ground states of target nuclei has been studied over a wide range of nuclear masses and bombarding energies, to obtain directly information about the isospin part of the optical potential. In contrast, relatively little work has been done on the reaction populating isobaric analogs of excited states, and these studies have been confined primarily to even-even nuclei with $A \lesssim 90$.¹⁻³ The reaction is found to populate selectively analogs of collective states with a cross section which is a significant fraction of that of the ground state (g.s.) analog. Except for light mirror nuclei, there has been only one reported observation of the (p, n) reaction to excited-state analogs in an odd- A nucleus.⁴ This lack of information is certainly partly due to the experimental difficulty of observing the fragmented strength above background which may be substantial for a heavy nucleus in a conventional, pulsed-beam, time-of-flight (TOF) experiment. Indeed, the lack of evidence for excited analogs in neutron TOF spectra has led one group to suggest⁵ that the reaction falls off strongly with mass number beyond $A = 90$.

In a heavy nucleus, the analog states are generally unbound and often a large fraction of the decay is by proton (\bar{p}) emission. Decay branches may be observed not only to the ground state, but also to excited states of the final nucleus. For example, in the reaction $^{119}\text{Sn}(p, n)^{119}\text{Sb}_{T_>}(\bar{p})^{118}\text{Sn}$,

analog of states in ^{119}Sn are formed in ^{119}Sb and these states can proton decay to states of ^{118}Sn . The energetics of the reaction are shown in Fig. 1. In ^{119}Sn , four states each contain a portion of the configuration formed by coupling an $s_{1/2}$ neutron to the 2^+ collective state of the core: the $\frac{3}{2}^+$ state at 0.920 MeV and three $\frac{5}{2}^+$ states at 0.921, 1.090, and 1.354 MeV. Proton decays following the (p, n') reaction to analogs of these states should fall into two energy groups: one at 8–8.5 MeV, corres-

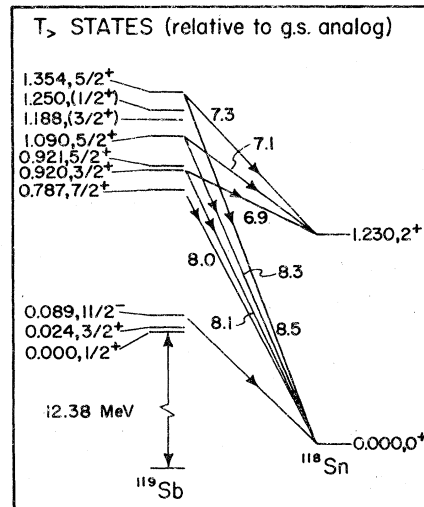


FIG. 1. Expected proton decay scheme (relative to the g.s. analog) of $T_>$ states in ^{119}Sb based on the known properties of the low-lying states of ^{119}Sn and ^{118}Sn (Refs. 23, 29, 31).

ponding to decays to the ground state of ^{118}Sn and a group, near 7 MeV, of decays to the 2^+ , 1.23 MeV state of ^{118}Sn . [The use of n' in the reaction notation (p, n') and $(p, n'\bar{p})$ is to indicate that the emitted neutron leaves the ^{119}Sb nucleus in the analog of an excited state of ^{119}Sn .]

Provided angular correlation effects are taken into account, the $(p, n'\bar{p})$ cross section is given by

$$\sigma(p, n'\bar{p}) = \sigma(p, n')\Gamma_p/\Gamma, \quad (1)$$

where Γ_p/Γ is the relative proton decay probability of the state reached in the (p, n') reaction. Therefore, if $\sigma(p, n')$ can be measured, one can obtain from the observed decays proton decay widths which are related to the spectroscopic factors for neutron transfer between the parent states (in ^{119}Sn) and daughter states (in ^{118}Sn). Unfortunately, as we will show, measuring $\sigma(p, n')$ directly on an odd- A nucleus as heavy as ^{119}Sn is extremely difficult, and it has not yet been done.

Observing the proton decay following the population of excited-state analogs in a (p, n') reaction is of interest for another reason. Anomalies have been reported⁶⁻⁸ in single detector measurements of \bar{p} decay following the (p, n) reaction on heavy nuclei, which may be attributed, at least in part, to "quasi-inelastic" scattering. Total \bar{p} yields were observed which are larger than expected on the basis of $\sigma(p, n)$ measurements^{5,9} and widths of the analog states were found to be greater than those determined from either (p, p') resonance studies^{10,11} or (p, n) TOF measurements.^{5,12}

If analogs of collective states are populated in the (p, n) reaction, the energy for their proton decay to the core-excited state in the final nucleus would be close to that for g.s. analog decay and would not be resolved from g.s. analog decay in a \bar{p} singles measurement. This is an example of the "window effect" first noted by Allan¹³ on the basis of his $^{118}\text{Sn}(p, p')^{118}\text{Sn}$ results. It was invoked by Grimes *et al.*⁹ to account in part for the discrepancy between the singles \bar{p} and (p, n) measurements on ^{208}Pb and ^{209}Bi . However, the great difficulty in observing the quasi-inelastic neutron peaks in the TOF spectra, and the speculation that the cross sections are small, meant that this possibility was open to question. In a measurement similar to that reported here, Bhowmik *et al.*¹⁴ report no significant evidence for excitation of excited analogs of ^{207}Pb and ^{208}Pb . They, however, make no calculations of the expected effect, which as we shall show for the case of ^{119}Sn , is small and could easily be hidden in their data.

In earlier papers,^{15,16} we described a technique for measuring quasi-elastic scattering on ^{119}Sn ,

in which the neutron from the (p, n) reaction was detected in coincidence with the decay proton. This technique is particularly well suited for looking for excited-state analogs, because the neutron background from reactions to the T_c states is greatly reduced. In this paper, we report observations of the (p, n) reaction to the excited-state analogs of ^{119}Sn described above, and their decays to states of ^{118}Sn . Population of the excited analogs is sufficiently large to account for a difference in Γ_p/Γ as measured in a singles \bar{p} experiment¹⁷ and in a recent comparison of coincidence and conventional TOF measurements of the g.s. analog yield.¹⁵

The (p, n') cross section was estimated from the data and the known spectroscopy of the nuclear states. A detailed analysis has been carried out in terms of a two-step reaction mechanism.¹⁸

II. EXPERIMENT

Data on the $^{119}\text{Sn}(p, n\bar{p})^{118}\text{Sn}$ reaction were taken using the n - p coincidence technique described in a previous paper.¹⁵ In a heavy nucleus ($A \geq 90$), analog (T_c) states are particle unstable and have a relatively high probability of decaying by proton (\bar{p}) emission. Thus, detecting a proton at the appropriate energy signaled that a $(p, n\bar{p})$ reaction may have taken place and the neutron TOF was determined relative to the proton signal. The coincidence method did not require a pulsed beam from the accelerator and yielded data of comparable quality to that obtained by (p, n) TOF methods.

The coincidence method has a significant advantage for the present work. Requiring a proton in coincidence with the neutron greatly reduced the background due to populating T_c states near the T_s state of interest, because the T_c states decay predominantly by neutron emission if it is energetically allowed. This reduction in neutron TOF background eliminated the need for good time-of-flight resolution and correspondingly long flight paths in the neutron detection arm. We have obtained relatively clean spectra at energies near reaction threshold, where the large background of evaporated neutrons makes the conventional method impractical.

A 2 mg/cm² ^{119}Sn target, enriched to 89.8% was bombarded with a proton beam from the University of Minnesota MP tandem Van de Graaff accelerator. Neutrons and γ rays were detected in an array of five 5 cm diam by 5 cm Ne 213 scintillators at 40 cm from the target. Conventional pulse shape discrimination (PSD) was used. Neutron TOF was determined relative to a charged-particle signal from either of a pair of surface-barrier detector telescopes placed at backward

angles. All coincident-pair events (charged-particle energy and neutron TOF) were recorded, event-by-event, on magnetic tape for extensive off-line reanalysis.

Data were taken at 36° , 48° , 60° , 72° , and 84° for incident energies covering the range 16–20 MeV in 1 MeV steps. More extensive angular distributions were taken at 17 MeV (36° – 156° in 6° steps) and 19 MeV (36° – 102° in 6° steps). These latter data form the basis for our present investigation.

III. RESULTS

A. Coincidence measurements

A proton-gated, TOF spectrum, taken at 48° and an incident energy of 17 MeV is shown in Fig. 2(a). The timing resolution was typically 1.7 nsec full width at half maximum (FWHM) and corresponds to 600 keV neutron energy resolution at $E_n = 3.2$ MeV. The peak labeled " γ " is due to γ events which were allowed to leak through the PSD window. In addition to the strong g.s. analog neutron peak at 3.2 MeV, labeled n_I , a lower energy group, n_{II} , appears in the energy region corresponding to populating analogs of states near 1 MeV in ^{119}Sn . The n_{II} group cannot be attributed to proton decays of T_z states in ^{119}Sb because these will decay mainly by the neutron channel, which opens at an excitation energy 2.8 MeV below that of the g.s. analog.

These data were analyzed off line by replaying the raw data tapes with the coincidence requirements reversed and extracting proton energy spectra gated by the neutron groups, n_I and n_{II} . The accidental background was obtained in a subsequent pass by gating on an appropriate region in the TOF spectrum, and was subtracted from each of the n_I - and n_{II} -gated spectra. Fig. 2(b) shows two such background-subtracted proton spectra.

The 7.2 MeV g.s. analog decay peak dominates the n_I -gated spectrum. Extracting this peak from the proton spectra was straightforward and an analysis and discussion of the g.s. analog data has already been reported.¹⁵ In the n_{II} -gated spectrum, several peaks are seen, corresponding to the decay of analogs of excited states of ^{119}Sn . The arrows in Fig. 2(b) indicate some of the expected proton decay energies based on the nature of low-lying states in ^{119}Sn (see Fig. 1). Peaks in the energy range 6.9–7.3 MeV correspond to the decay of analogs of excited states between 0.92 and 1.35 MeV to the 1.23 MeV, 2^+ state in ^{118}Sn . Some evidence is seen in the 8.0–8.5 MeV region for decays to the g.s. of ^{118}Sn .

The yields due to excited-state analog decays

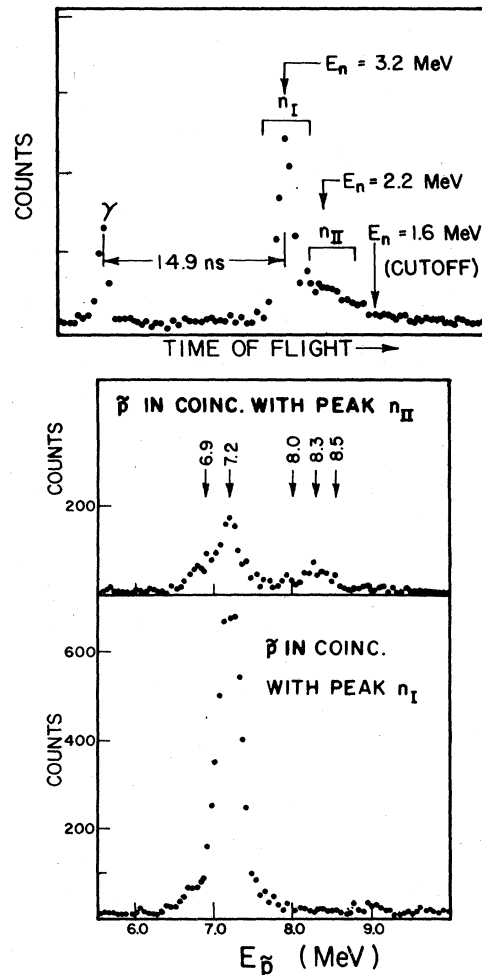


FIG. 2. (a) Neutron time-of-flight spectrum for the reaction $^{119}\text{Sn}(p, n\bar{p})^{118}\text{Sn}$ at 48° and incident energy of 17 MeV, gated by protons. The neutron groups correspond to population of analogs of the ^{119}Sn g.s. (n_I) and states at an excitation energy near 1 MeV (n_{II}). Also shown are a γ peak and the detector threshold corresponding to 1.6 MeV neutrons. (b) Decay proton spectra in coincidence with the neutron groups n_I (lower) and n_{II} (upper), after background subtraction. The arrows indicate several probable proton energies following the population of excited analogs of ^{119}Sn and their decays to either the ground or first excited states of ^{118}Sn .

to the $^{118}\text{Sn}(2^+)$ state were obtained by a graphical fit to the peak shapes. The group near 7.2 MeV in the n_{II} -gated spectrum undoubtedly contains some contribution from the g.s. analog decay. This was estimated from an analysis of a series of proton spectra obtained by gating on narrow bands of neutron energies across the TOF region containing n_I and n_{II} . The excited-state analog groups in the 6.9–7.3 MeV region could not be resolved adequately one from another, so the net yield from *all* the contributing decays in this re-

gion was estimated for each spectrum. In what follows, it is this group of decays which will be termed the "excited state analog yield."

Differential cross sections were determined from these net yields. The calculations included corrections for finite solid angle effects in both the neutron and proton detectors. An overall scale uncertainty of $\pm 8\%$ for the excited states analog cross section at 19 MeV results from uncertainties in the neutron detection efficiency ($\pm 7\%$), attenuation in the scattering chamber wall ($\pm 2\%$) and target thickness ($\pm 2\%$). At 17 MeV, the outgoing neutrons from the excited-state analog reactions have energies near 2 MeV, which is in the region where the neutron detection efficiency rises steeply with energy from threshold (1.6 MeV). The efficiency is not well known near threshold, and as a result, the 17 MeV cross sections have a scale uncertainty of at least $\pm 20\%$. The angular distributions for the excited-state analogs at 17 and 19 MeV are shown in Fig. 3. These angular distributions have been plotted as a function of c.m. neutron angle. In principle, they depend also on the angle of the emitted proton; however, the analogs of excited states decay to the ^{118}Sn 2^+ state largely via $l=0$. Thus, the n - p angular correlation will be essentially isotropic and the observed yield can be written in the form of Eq. (1).

It was not possible to obtain useful angular distributions for the excited-state analog decays to

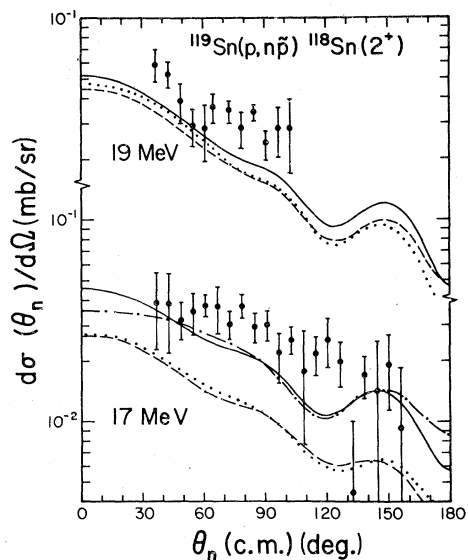


FIG. 3. Angular distributions taken at 17 and 19 MeV of the $(p, n\bar{p})$ excited-state analog yield via the analogs of the four states listed in Table I. The curves are two-step DWBA calculations using the coupling scheme of Fig. 6(a) as described in the text.

the ^{118}Sn ground state. Their yield typically was 10–15% of that seen for decays to the 2^+ state, and, in most cases, it was difficult to distinguish *bona fide* peaks from background in the 8.0–8.5 MeV region of the proton spectra.

B. Comparison with (p, n) time-of-flight data

As part of the study of the $^{119}\text{Sn}(p, n)$ g.s. analog reaction,¹⁵ data were taken at Lawrence Livermore Laboratory using a conventional, pulsed-beam TOF method. Spectra obtained in long runs with correspondingly good statistics were examined for evidence of population of excited-state analogs. Figure 4 shows a portion of one of these TOF spectra. (Note the suppressed zero for the ordinate.) The g.s. analog peak is clearly visible, but, in contrast to the coincidence spectrum of Fig. 2(a), there is a substantial background due to (p, n) reactions proceeding to T_c states in ^{119}Sb . While this background makes identification of the excited-state analog peaks rather tenuous, the data are consistent with the presence of such peaks having the relative strengths of those determined in the n - \bar{p} coincidence measurements. This is shown in Fig. 4, where the g.s. analog peak shape,

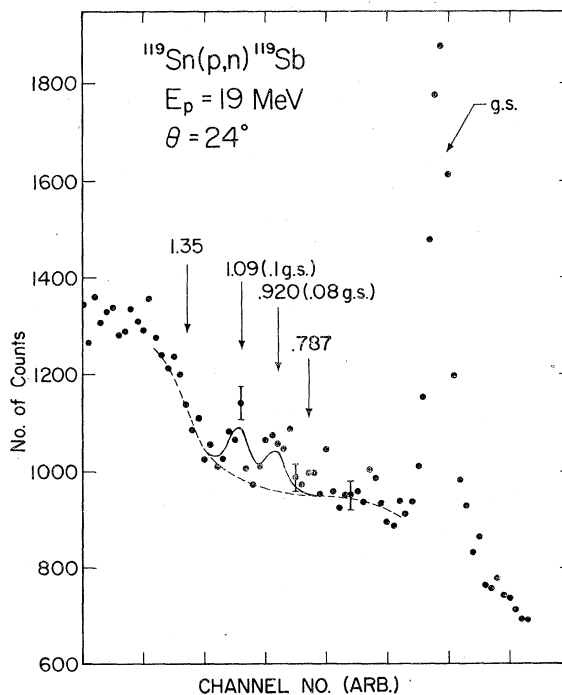


FIG. 4. Portion of a conventional pulsed-beam, time-of-flight spectrum for the $^{119}\text{Sn}(p, n)^{119}\text{Sb}$ reaction at 24° and 19 MeV bombarding energy showing the g.s. (IAS) peak and the positions of several excited analogs. The solid curve is an estimate of the yield to the 1.09 and 0.920 MeV analogs based on the n - \bar{p} coincidence data.

reduced by the indicated factors of 0.10 and 0.08, has been added to a smooth background (dotted curve) at flight times corresponding to excitation energies, respectively, of 1.09 and 0.92 MeV above the g.s. analog. These reduction factors were estimated from the ratio of the excited and g.s. analog yields seen in the coincidence experiment. They are appropriate because, as is discussed later, the relative proton decay widths of the excited-state analog group and the g.s. analog are approximately equal. Although the error bars on the data points are large, there is evidence for analogs of excited states at 0.92 and 1.09 MeV. Analogs of excited states at 0.787 and 1.35 MeV appear to be less strongly excited.

C. Decay of the excited-state analogs

The coincidence data show that analogs of excited states between 0.92 and 1.35 MeV decay preferentially to the 1.23 MeV (2^+) state of ^{118}Sn , indicating that these analog states contain significant fractions of the 2^+ core excitation. This agrees with the general finding of experiments on lighter nuclei¹⁻⁴ that quasi-inelastic scattering selectively populates analogs of collective states.

The observations also are an example of the "window" effect, first pointed out by Allan,¹³ who noted that the majority of protons from the decay of excited analogs in ^{119}Sb have energies close to that of the g.s. (IAS) \rightarrow g.s. decay. In the present case, the excited-state analog decay energies are within 100–300 keV of the g.s. analog decay energy of 7.2 MeV, and would not be resolved from the

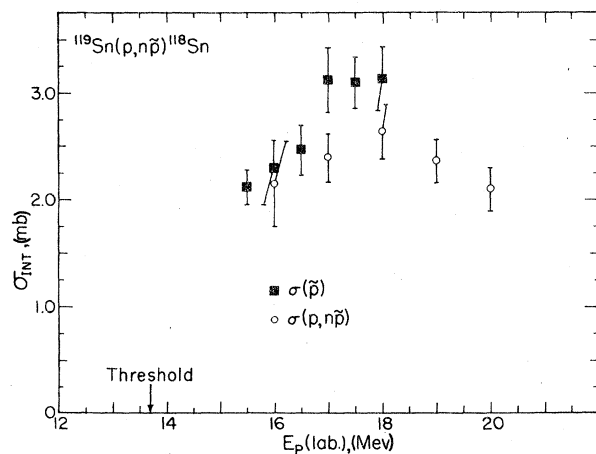


FIG. 5. Total $^{119}\text{Sn}(p, n\tilde{p})^{118}\text{Sn}$ cross section plotted as a function of bombarding energy. Circles are the data of Ref. 15 for excitation and decay of the ^{119}Sn g.s. analog only. Squares are the results of Ref. 17 for the yields of protons with energies near 7.2 MeV as measured in a single detector experiment.

latter in a single proton detector experiment.

In Fig. 5, $\sigma(p, n)\Gamma_p/\Gamma$ values for the g.s. analog reaction as determined from the single detector \tilde{p} measurements of Miller and Garvey,¹⁷ are compared, as a function of energy, with the published results of our $n\tilde{p}$ coincidence experiment.¹⁵ As can be seen, the agreement between the two methods is good at 16 MeV, but at 17 and 18 MeV the \tilde{p} results (solid squares) are about 25% larger than those of the $n\tilde{p}$ coincidence experiment (open circles). The disagreement is approximately the same as the ratio, seen in our measurements, of the integrated yield for the excited state analogs to that for the g.s. analog and accounts for the larger value of Γ_p/Γ (0.38 ± 0.05) quoted in Ref. 17 compared with that (0.34) determined from (p, p') resonance scattering¹⁹ or from a direct comparison of $n\tilde{p}$ coincidence and (p, n) TOF data (0.320 ± 0.015).¹⁵

IV. ANALYSIS AND DISCUSSION

An early attempt²⁰ to interpret quasi-inelastic scattering as a one-step process analogous to inelastic scattering, by deforming the isospin potential gave cross sections which were an order of magnitude smaller than those observed. Later, in 1972, Madsen *et al.*¹⁸ showed that the (p, n') cross section for transitions to analogs of strongly collective states proceeds primarily via a two-step mechanism of inelastic excitation of the core collective state, followed by charge exchange, or vice versa. The direct one-step amplitude not only is relatively small, as noted above, but is 90° out of phase with the two-step amplitudes and may be neglected. A coupled-channel method²¹ was used to solve the Schrödinger equation, including the g.s., the core-excited state of the target and their analogs as four coupled states. This description was extended to (p, n') analog reactions on the odd- A target ^{63}Cu ,⁴ using the weak-coupling model²² to describe the fragmentation of the core state due to particle-vibration coupling.

In the two-step model of quasi-inelastic scattering, the overall reaction amplitude is proportional to the amplitude for the inelastic step. Thus the analog of an excited state in ^{119}Sn (Fig. 1) will be seen only if it has appreciable collective strength. In ^{119}Sn , the three $\frac{5}{2}^+$ states at 0.921, 1.09, and 1.35 MeV and the $\frac{3}{2}^+$ state at 0.920 MeV are seen strongly in Coulomb excitation and account for the strength of the 2^+ core vibration coupled to an $s_{1/2}$ neutron.²³ Properties of these states are given in Table I. The tabulated values of the deformation parameter β_2 were calculated from measured $B(E2)$ values,²³ assuming a uni-

TABLE I. $B(E2)$ values from Coulomb excitation and deformation parameters for states in ^{119}Sn .

Excitation Energy (MeV) ^a	J^π	$B(E2)^a$ ($e^2\text{fm}^4$)	β_2
0.920	$\frac{3}{2}^+$	720 ± 70	0.0645 ± 0.0031
0.921	$\frac{5}{2}^+$	600 ± 75	0.0589 ± 0.0037
1.090	$\frac{5}{2}^+$	310 ± 15	0.0423 ± 0.0010
1.354	$\frac{5}{2}^+$	230 ± 15	0.0365 ± 0.0012

^aFrom Ref. 23.

formly charged sphere of radius $1.4A^{1/3}$. Other excited states in ^{119}Sn were seen weakly or not at all in Coulomb excitation, and no evidence was found for the population of their analogs in the present experiment.

Contributions arising from a single-particle exchange mechanism (SPE) of neutron pickup followed by proton stripping were assumed to be small in the present case, although they have been claimed to be important in charge exchange reactions in certain other cases. The greatest success of the SPE mechanism has apparently been in reproducing the cross sections for the ($^3\text{He}, t$) reaction to the analog of the target ground state²⁴ and to antianalog states.²⁵ Including the (p, d)(d, n) contribution also resulted²⁶ in improved agreement of calculated and measured (p, n) angular distributions for the g.s. analog reaction. However, these SPE calculations were all performed in the zero-range approximation, and recently Kunz and Charlton have shown^{27,28} that first order finite-range corrections in SPE calculations are extremely large and opposite in phase to the zero-range term. Accordingly, when the calculations are performed in full finite range, the SPE contribution is reduced substantially compared to the zero-range calculations. It appears, therefore, that the contribution of SPE to charge exchange reactions is smaller than it was formerly believed to be in these cases.

Secondly, in ($^3\text{He}, t$), SPE forms an α particle in the intermediate state. This releases a large amount of energy to the system, and so there are many coherent intermediate states which are accessible. In (p, n) on the other hand, SPE takes place via an intermediate deuteron which is loosely bound and so the energetics are less favorable for its formation.

Finally, SPE would be expected to populate single-particle configurations rather than collective states. Experimentally,⁴ it is observed that the (p, n') reaction strongly populates analogs of collective states, nearly to the exclusion of single-

particle states. Therefore, even if SPE did contribute to charge exchange in cases where the overlap with single-particle states is strong, the SPE contribution to (p, n') would be small.

The observation of the collective state selectivity of the (p, n') reaction is supported by the present results. The 0.79 MeV, $\frac{7}{2}^+$ state in ^{119}Sn is described as a relatively pure $f_{7/2}$ single quasi-particle (SQP) state. Its strength as seen in the (d, p) reaction²⁹ is 2–6 times that of the states listed in Table I. However, its analog was not observed to be populated in the present ($p, n'\bar{p}$) studies, and, hence, population of the $\frac{5}{2}^+$ states of Table I via their $d_{5/2}$ SQP components was ignored in the present analysis.

In order to compare the excited analog yields with calculations, an estimate was made of the relative proton decay width of the excited analog group. For each analog state, the decay depends on its overlap with states of ^{118}Sn , the orbital angular momentum carried away by the decay proton, and its energy relative to the height of the Coulomb barrier.

In the decay of a $\frac{3}{2}^+$ or $\frac{5}{2}^+$ IAS to the 0^+ (g.s.) of ^{118}Sn only angular momentum transfer $l=2$ is allowed, whereas $l=0, 2,$ and 4 are allowed for decay to the 2^+ state. The energies are such that the transmission coefficient for the $l=2$ g.s. decay ($\bar{E}_p \sim 8.2$ MeV) is essentially the same as that for the $l=0$ decay to the 1.23 MeV (2^+) state ($\bar{E}_p \sim 7.0$ MeV). [In fact, $T_2(8.2 \text{ MeV}) = 0.34$, whereas $T_0(7.0 \text{ MeV}) = 0.33$.³⁰] Furthermore, both of these are nearly equal to the transmission coefficient of the $l=0$ g.s. (IAS)–g.s. decay [$T_0(7.2 \text{ MeV}) = 0.35$ (Ref. 30)]. Differences in partial proton widths Γ_p for these decay modes, therefore, must be attributed almost entirely to differences in overlap between the parent analog and daughter states.

The structure of the states given in Table I is such that their analogs can only decay via $l=0$ to the 2^+ state of ^{118}Sn . Spectroscopic factors for $l=2$ or $l=4$ decays would require admixtures of d and g orbitals coupled to the 2^+ core state, and these are expected to be small. In addition, the transmission coefficients for $l=2$ and 4 decays (0.15 and 0.02,³⁰ respectively) are reduced relative to $l=0$ (0.33). Consequently, these facts support the assumption that the excited (IAS)– 2^+ decay is essentially pure $l=0$, and that the ($p, n'\bar{p}$) cross section is given by Eq. (1).

Because the $l=0$ penetrabilities of the excited (IAS)– 2^+ and g.s. (IAS)–g.s. decays are similar, the partial proton width of the former, $\Gamma_p(\text{exc} \rightarrow 2^+)$, for each excited analog is related, via the strength of its ($2^+ \otimes s_{1/2}$) component, to that of the latter; $\Gamma_p(\text{g.s. IAS})$. In an extreme weak-coupling picture,

there would be only one $\frac{3}{2}^+$ state and one $\frac{5}{2}^+$ state formed by coupling an $s_{1/2}$ neutron to a 2^+ core excitation, and $\Gamma_p(\text{exc} \rightarrow 2^+)$ and $\Gamma_p(\text{g.s. IAS})$ would be equal. The partial proton width and the total width, Γ , for the g.s. analog have been measured to be 17 and 50 keV, respectively.¹⁹

This simple picture is somewhat complicated in ^{119}Sn by the mixing of nearby single quasiparticle (SQP) levels. In particular, the SQP energy for $d_{5/2}$ is 1.43 MeV,²⁹ with the result that the $\frac{3}{2}^+$ weak-coupling state is fragmented into levels at 0.921, 1.09, and 1.35 MeV, all of which contain some $d_{5/2}$ admixture as is seen in stripping reactions.^{29,31} Thus, the proton decay width of the $\frac{5}{2}^+$ weak-coupling state is divided among the three states, with the 0.921 MeV state taking the biggest fraction. The total width, Γ , of each of the excited analogs may be taken to be similar to the measured value¹⁹ of 37 keV for the 1.09 MeV $\frac{5}{2}^+$ state. With these numbers it was estimated that $(p, n' \bar{p})$ accounts for approximately one-third of the total (p, n') yield to the four excited analog states.

Using these simple arguments it is qualitatively easy to understand the relatively low exc (IAS) \rightarrow g.s. decay probability observed in the present experiment. Assuming that quasi-elastic scattering proceeds via the core-excited components of the final state, the majority of the yield will be to states at 0.920 and 0.921 MeV, which have rather small overlaps with the 0^+ ground state.

The two-step model was applied to the excited-state analog transitions which were observed at bombarding energies of 17 and 19 MeV. Two sets of calculations were carried out using the computer code CHORK.³² These are indicated schematically in Fig. 6 for the $\frac{3}{2}^+$ state. In Fig. 6(a)

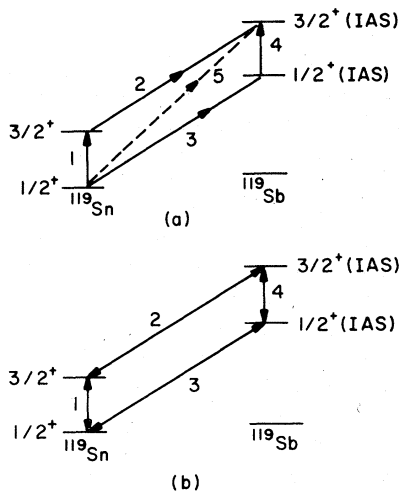


FIG. 6. Channel coupling schemes used in the one-way coupling (a) and full coupling (b) calculations.

TABLE II. Optical model parameters. Parameters are those of Ref. 34: $\gamma = Z/A^{1/3}$, $\epsilon = (N-Z)/A$, W_p and $W_s \geq 0$ always. All potentials are in MeV and all distances are in fm.

V^p	$55.2 - 0.32 E_p + 0.27\gamma + 24\epsilon$
W_p^p	$0.22 E_p - 0.18\gamma - 1.4$
W_s^p	$10.2 - 0.25 E_p + 0.21\gamma + 12\epsilon$
V^n	$55.2 - 0.32 E_n - 24\epsilon$
W_p^n	$0.22 E_n - 1.4$
W_s^n	$12.0 - 0.25 E_n - 12\epsilon$
	$R_R^p = R_R^n = 1.17$, $a_R^p = a_R^n = 0.75$
	$V_{so} = 6.2$, $R_{so} = 1.01$, $a_{so} = 0.75$
	$R_I^p = 1.32$, $a_I^p = 0.51 + 0.7\epsilon$, $R_I^n = 1.26$, $a_I^n = 0.58$

the couplings are one-way, so the paths (1+2) and (3+4) are equivalent to two-step DWBA calculations. In Fig. 6(b) full channel coupling is used. In three of the one-way coupling calculations only the two-step paths (1+2) and (3+4) were considered; in one calculation, the direct path was included. The three calculations illustrate slightly different parametrizations of the optical potential, which were used previously in describing fits to the quasi-elastic data.¹⁵ They will be referred to as sets A, B, and C, and are all consistent with or are close to being consistent with the Lane representation of the optical potential.³³

These potentials are based on the " $V_{cc} = 0.84$ " proton parameters and "common" neutron parameters of Ref. 34, which are given in Table II. The form of either the neutron or proton potential is given by

$$\begin{aligned}
 U(r) = & -V_R f(r, r_R, a_R) - iW_v f(r, r_I, a_I) \\
 & + i4a_I W_s \frac{df}{dr}(r, r_I, a_I) \\
 & + V_{so} \chi_\pi^2 \frac{(\vec{\sigma} \cdot \vec{1})}{r} \frac{df}{dr}(r, r_{so}, a_{so}) + V_C(r, r_C) \\
 = & -U_o(r) + \frac{4}{A} \vec{t} \cdot \vec{T} U_I(r), \quad (2)
 \end{aligned}$$

where $f(r, r_i, a_i) = [1 + \exp(r - r_i^{1/3})/a_i]^{-1}$ and V_C is the Coulomb potential due to a uniformly-charged sphere. Both sets A and B use the parameters of Table II as given, but the charge-exchange form factor is calculated differently for the two cases. For set A it was assumed that $U_{pn}(r) \propto U_I(r)$, where the strength, U_I , and geometry parameters were taken from the optical potentials. Because a_I and r_I are slightly different for protons than they are for neutrons, average values were used for these parameters in the form factor. For set B, the difference in neutron and proton geometries was accounted for by calculating $U_{pn}(r)$ according to the

Lane model, from the difference of the neutron and proton optical potentials at each value of the radius. That is, at each value of r , $U_{pn}(r)$ was calculated according to

$$U_{pn} = (N - Z)^{-1/2}(U_n - U_p). \quad (3)$$

Set C differs from set B only in that all imaginary terms in the neutron potential are reduced by a factor F which depends on the neutron energy E_n . Ref. 15 contains a full discussion of the considerations under which the parameter sets were chosen.

As is discussed in Ref. 15, sets A, B, and C predict different quasielastic scattering angular distributions. Those of set A underestimate the total cross section for bombarding energies below about 19 MeV, and also incorrectly describe the shape at forward angles. Calculating the charge-exchange potential with Eq. (3) in set B, improves the forward-angle shape, but still underestimates the cross section in the same way as set A. By reducing the imaginary neutron potential in set C, good overall fits were obtained at all energies. The factor F was found to decrease from unity at 20 MeV to 0.6 at 16 MeV,¹⁵ and gives a more realistic energy dependence to the neutron imaginary potential than is given by that of set A or B. This reduced potential also gave significantly improved fits to low-energy neutron elastic scattering and reaction data.

The results of the two-step DWBA calculations are presented in Fig. 3. Each predicted angular distribution is the sum of contributions to analogs of the four states of Table I scaled by the estimated proton decay probability (0.32). There are no free parameters for the (p, n') calculation: These were determined from the (p, n) reaction, neutron scattering, and Coulomb excitation data. Set A (dotted curve) and set B (dashed curve) are similar in both magnitude and shape at both energies. At 19 MeV there is reasonable agreement with the magnitude of the cross section, whereas at 17 MeV considerable improvement is given by set C (solid curve). Thus, while the difference in the shapes of the forward-angle quasi-elastic angular distribution predicted by sets A and B are not seen in the quasi-inelastic predictions, the same factor F which was required to reproduce the magnitude of the quasi-elastic cross section is needed to achieve agreement here. Considering the approximations used in the description and in estimating the overall relative proton decay probability for the excited analog states, the agreement with the data is satisfactory.

Calculations also have been carried out using the Lane-consistent optical potential recently obtained from a global fit to (p, n) data.³⁵ The results are essentially the same as those of set A. The agreement with the 19 MeV data is good, but the 17 MeV data are underestimated.

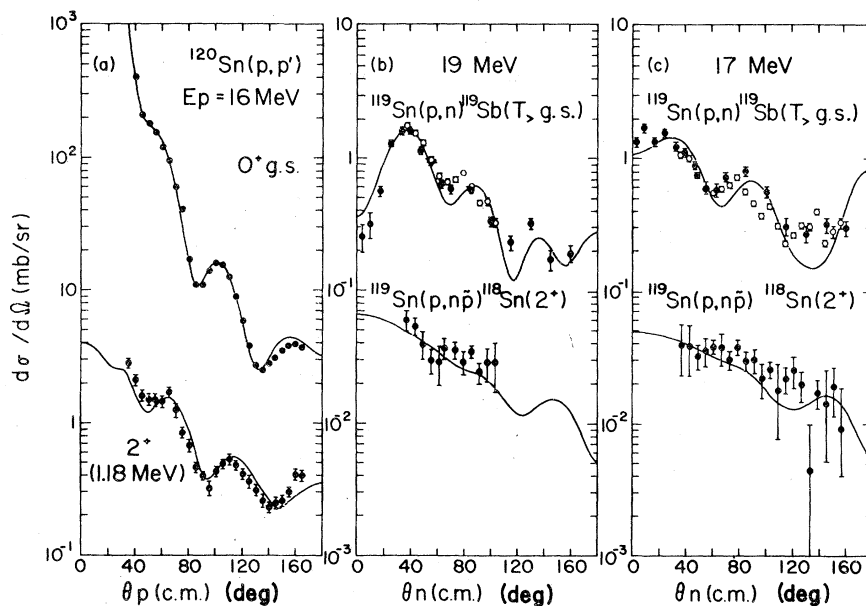


FIG. 7. Results of coupled-channels calculations using the coupling scheme of Fig. 6(b) compared with the following: (a) $p + {}^{120}\text{Sn}$ elastic scattering and inelastic scattering to the first excited 2^+ state taken at 16 MeV (Ref. 36). (b) Differential cross sections for ${}^{119}\text{Sn}(p, n){}^{119}\text{Sb}$ (g.s. IAS) and ${}^{119}\text{Sn}(p, \tilde{n}){}^{118}\text{Sn}(2^+)$ reactions at 19 MeV. The open circles are the (pn, \tilde{p}) data for decay to the g.s. analog scaled as described in Ref. 15 to the (p, n) data (closed circles, upper curve) taken by TOF. (c) Same as (b) for 17 MeV.

The effect of including the direct term (path 5) is minor and is shown only for 17 MeV. The contribution of this path alone varies from a few to ten percent of the two-step cross section. However, when it is included in a full calculation its effect is small, as is shown in Fig. 3 by the dot-dashed curve, which is a calculation using set C. Thus the direct amplitude appears to add incoherently as was found previously.¹⁸

Figure 7 summarizes the full coupled-channels calculations corresponding to Fig. 6(b). They are shown only for one optical potential since the effect of changing the potential parametrization is similar to that exhibited by the two-step DWBA calculations just described. Set C parametrization was used and the effect of channel coupling on the absorption potentials was estimated by a comparison to 16 MeV elastic and inelastic $p + {}^{120}\text{Sn}$ data of Makofske *et al.*³⁶ Good agreement of a coupled-channels calculation with these data was obtained by reducing all the imaginary strengths by 12%, as is shown in Fig. 7(a). This reduction in all absorption potentials was applied in the coupled channels calculation for the (p, n) and (p, n') reactions.

Figures 7(b) and 7(c) compare the resulting quasi-elastic calculation with data. The shapes are essentially the same as the DWBA calculations of Ref. 15 which neglected channel coupling. This is in contrast to recently published results for the molybdenum isotopes³ which showed that channel coupling had a large effect. This is presumably a direct result of the size of the deformation parameter β_2 which is considerably larger for several of the molybdenum isotopes than it is for the tin isotopes. This interpretation is consistent with

the results of Ref. 3 for ${}^{92}\text{Mo}$, which has a small deformation parameter ($\beta_2 \sim 0.08$) and for which the effects of channel coupling on the g.s. analog are small.

Finally, the coupled-channels quasi-inelastic predictions are compared to the data in Figs. 7(b) and 7(c). As previously discussed, there are no free parameters in these calculations. Agreement between prediction and experiment is excellent.

In summary, it appears that quasi-inelastic (p, n) scattering on ${}^{119}\text{Sn}$ preferentially excites analogs of collective states and can be well described by the two-step model of Madsen *et al.*¹⁸ Changes in the imaginary strength of the neutron potential which improved the description of the quasi-elastic scattering near threshold also were necessary to achieve good agreement to quasi-inelastic scattering. The effect of full channel coupling was minor, provided the absorptive potentials were adjusted to fit elastic and inelastic scattering. The analogs of the excited states of ${}^{119}\text{Sn}$ populated in these studies proton decay overwhelmingly to the first excited 2^+ state of ${}^{118}\text{Sn}$. Their proton decay energies are close to that of the g.s. (IAS) decay and their overall yield accounts for the observed difference between singles \bar{p} and $(n-\bar{p})$ coincidence measurements of the $(p, n\bar{p})$ cross section via the g.s. IAS.

More information could be obtained from these studies if the proton detector resolution were improved, and particularly if the (p, n') cross sections could be determined. Determining the individual proton decay branches of the analog states would enable a much more critical test to be made of the assumed reaction mechanism.

† Work performed under the auspices of the U. S. Department of Energy by the University of Minnesota under Contract No. E(11-1)-1265 and the Lawrence Livermore Laboratory under Contract No. W-7405-Eng-48.

* Present address: Crocker Nuclear Laboratory and Department of Physics, University of California, Davis, California 95616.

‡ Present address: Nuclear Structure Facility, Daresbury Laboratory, Daresbury, Warrington, WA4 4AD, England.

§ Present address: Lawrence Livermore Laboratory, Livermore, California, 94550.

¹J. D. Anderson and C. Wong, *Phys. Rev. Lett.* **8**, 442 (1962).

²J. D. Anderson, C. Wong, J. W. McClure, and B. D. Walker, *Phys. Rev.* **136**, B118 (1964).

³V. A. Madsen, V. R. Brown, S. M. Grimes, C. H. Poppe, J. D. Anderson, J. C. Davis, and C. Wong, *Phys. Rev. C* **13**, 548 (1976).

⁴C. Wong, V. R. Brown, J. D. Anderson, J. C. Davis, S. M. Grimes, C. H. Poppe, and V. A. Madsen, *Phys. Rev. C* **11**, 137 (1975).

⁵H. W. Fielding, S. D. Schery, D. A. Lind, C. D. Zafiratos, and C. D. Goodman, *Phys. Rev. C* **10**, 1560 (1974); and S. D. Schery, D. A. Lind, H. W. Fielding, and C. D. Zafiratos, *Nucl. Phys.* **A234**, 109 (1974).

⁶G. M. Crawley and P. S. Miller, *Phys. Rev. C* **6**, 306 (1972).

⁷G. M. Crawley, W. Benenson, P. S. Miller, D. L. Bayer, R. St. Onge, and A. Kromminga, *Phys. Rev. C* **2**, 1071 (1970).

⁸G. W. Hoffmann, W. H. Dunlop, G. J. Igo, J. G. Kulleck, J. W. Sunier, and C. A. Whitten, Jr., *Nucl. Phys.* **A187**, 577 (1972).

⁹S. M. Grimes, J. D. Anderson, J. C. Davis, W. H. Dunlop, and C. Wong, *Phys. Rev. Lett.* **30**, 992 (1973).

¹⁰C. D. Kavaloski, J. S. Lilley, P. Richard, and N. Stein, *Phys. Rev. Lett.* **16**, 807 (1966); G. M. Temmer, G. H. Lenz, and G. T. Garvey, in *Proceedings of the*

- International Conference on Nuclear Physics*, edited by R. L. Becker, C. D. Goodman, P. H. Stelson, and A. Zucker (Academic, N.Y., 1967), p. 255.
- ¹¹B. L. Anderson, J. B. Bondorf, and B. S. Madsen, Phys. Lett. 22, 651 (1966); G. H. Lenz and G. M. Temmer, Nucl. Phys. A112, 625 (1968); G. W. Bund and J. S. Blair, *ibid.* A144, 384 (1970).
- ¹²G. M. Crawley, P. S. Miller, A. Galonsky, T. Amos, and R. Doering, Phys. Rev. C 6, 1890 (1972).
- ¹³D. L. Allan, Phys. Lett. 14, 311 (1965).
- ¹⁴R. Bhowmik, R. R. Doering, A. Galonsky, and P. S. Miller, Z. Phys. A280, 267 (1977).
- ¹⁵D. H. Fitzgerald, G. W. Greenlees, J. S. Lilley, C. H. Poppe, S. M. Grimes, and C. Wong, Phys. Rev. C 16, 2181 (1977).
- ¹⁶D. H. Fitzgerald, G. W. Greenlees, J. S. Lilley, J. M. Moss, and T. Woods, Phys. Rev. Lett. 34, 890 (1975).
- ¹⁷P. S. Miller and G. T. Garvey, Nucl. Phys. A163, 65 (1971).
- ¹⁸V. A. Madsen, M. J. Stomp, V. R. Brown, J. D. Anderson, L. Hansen, C. Wong, and J. J. Wesolowski, Phys. Rev. Lett. 28, 629 (1972).
- ¹⁹P. Richard, C. F. Moore, J. A. Becker, and J. D. Fox, Phys. Rev. 145, 971 (1966).
- ²⁰G. R. Satchler, R. M. Drisko, and R. H. Bassel, Phys. Rev. 136, B637 (1964).
- ²¹B. Buck, Phys. Rev. 130, 712 (1963).
- ²²A. de-Shalit, Phys. Rev. 122, 1530 (1961).
- ²³P. H. Stelson, W. T. Milner, F. K. McGowan, R. L. Robinson, and S. Raman, Nucl. Phys. A190, 197 (1972).
- ²⁴Manabu Toyama, Nucl. Phys. A211, 254 (1973).
- ²⁵R. Schaeffer and G. Bertsch, Phys. Lett. 38B, 159 (1972).
- ²⁶L. D. Rickertson and P. D. Kunz, Phys. Lett. 47B, 11 (1973).
- ²⁷P. D. Kunz and L. A. Charlton, Phys. Lett. 61B, 1 (1976).
- ²⁸L. A. Charlton and P. D. Kunz, Phys. Lett. 72B, 7 (1977).
- ²⁹E. J. Schneid, A. Prakash, and B. L. Cohen, Phys. Rev. 156, 1316 (1967).
- ³⁰Proton transmission coefficients were obtained using the standard optical model and the best fit proton potential parameters of Ref. 34.
- ³¹T. Borello-Lewin, C. Q. Orsini, O. Dietzsch, and E. W. Hamburger, Nucl. Phys. A249, 284 (1975).
- ³²L. D. Rickertson, private communication.
- ³³A. M. Lane, Phys. Rev. Lett. 8, 171 (1962); Nucl. Phys. 35, 376 (1962).
- ³⁴F. D. Becchetti, Jr. and G. W. Greenlees, Phys. Rev. 182, 1190 (1969).
- ³⁵D. M. Patterson, R. R. Doering, and A. Galonsky, Nucl. Phys. A263, 261 (1976).
- ³⁶W. Makofske, W. Savin, H. Ogata, and T. H. Kruse, Phys. Rev. 174, 1429 (1968).